*Progress In Electromagnetics Research C, Vol. 69, 1–10, 2016*

# Dynamic Wireless Charging for Roadway-Powered Electric Vehicles: A Comprehensive Analysis and Design

**Bin Deng, Bingnan Jia, and Zhen Zhang***

**Abstract**—This paper presents a comprehensive analysis of the roadway powering system for electric vehicles (EVs) and proposes a design from the perspective of power track design, integration, and powering control strategy, aiming to ensure the charging power and persistence, enhance the control flexibility, and reduce the construction cost. 1) A novel design scheme is first proposed to determine the length and number of turns for power tracks by investigating the power supply-and-demand and the loss. 2) A novel evaluation index, namely the magnetic distribution variance, is proposed to determine the gap between adjacent tracks, which can effectively produce evenly-distributed energy field, thus improving the dynamic charging performance for EVs. 3) A sectional powering control strategy is proposed to implement a cost-saving and flexible roadway powering system. Lastly, the simulated and experimental results show that the exemplified prototype can achieve the transmission power 50 W over the distance of 200 mm, which verifies the proposed EV dynamic charging system with the salient advantages of the constant energization, flexible power control, and cost saving.

## 1. INTRODUCTION

By penetrating renewable energies into our daily life, electric vehicle (EV) shows salient significance for relieving the crisis of the traditional energy as well as alleviating the environmental issues [1]. With the advantages of the utilization of clean energies, the EV undoubtedly will predominate the future transportation. Nevertheless, due to the current battery technique, namely the low energy density, short lifetime and high cost, the corresponding energy storage has inevitably become a technical bottleneck, which significantly impedes the further popularization of EVs.

As an emerging technique, inductive power transfer (IPT) can transmit the energy via the induced electromagnetic field [2]. From the perspective of EVs, the cordless energy transmission technique can effectively increase the driving range due to limited battery storage and save the cost due to installation of a large number of batteries. Accordingly, it has been increasingly taken as a preferable technique to bypass the current battery limits, thus further facilitating the development and improving the market acceptance for EVs. In previous studies [3–5], the EV wireless charging can be classified as the static and dynamic EV charging mechanisms.

For EV static wireless charging systems, IPT was elaborately discussed in terms of the theoretical and practical design issues [6]. From the perspective of the coil design, a new polarized coupler topology was presented to improve the position-tolerant performance for IPT systems [7]. Then, the fundamental design of the bipolar magnetic coupler was introduced for the primary control [8]. In [9], a contactless charging system based on a circular coil configuration was presented for EVs. In recent years, the EV dynamic charging has attracted increasing attention. For example, a new cross-segmented power supply rail was proposed for roadway-powered EVs to control the current direction of a pair of power cables as well as reduce the construction cost [10]. The self-decoupled dual pick-up coils were also presented to enhance the lateral tolerance for the charging performance and reduce the

*Received 11 July 2016, Accepted 2 October 2016, Scheduled 26 October 2016*
* Corresponding author: Zhen Zhang (zhangz@tju.edu.cn).
The authors are with the School of Electrical Engineering & Automation, Tianjin University, China.

low electromagnetic field for the pedestrian health [11]. Additionally, a contactless charging IPT system using inductive loops connected to a resonance converter was designed for EVs [12]. Also, the use of inductive links to wirelessly power an autonomous sensor was proposed in a vehicle application [13]. Besides, by using an economic model of battery size and charging infrastructure allocation, the economic analysis was quantitatively carried out with emphasis on the benefits of dynamic charging [14]. For the exemplification project of the EV dynamic charging, in particular, KAIST has made fruitful achievements on On-Line Electric Vehicle (OLEV) [15], which verifies the feasibility of the dynamic charging mechanism and offers significant technical basis for the future development. By comparing with EV static charging systems, the dynamic charging can offer a flexible energization way for moving EVs. Specifically, the moving EV can harness the energy in the air, which effectively alleviates the dependence on the battery. Thus, the dynamic charging scheme can significantly reduce the cost and weight as well as increasing the driving range for EVs.

As aforementioned, previous studies mainly focus on specific components, such as coil design and economic analysis, while the comprehensive analysis has been nearly unexplored for the dynamic charging mechanism, especially for the impacts of the vehicle velocity, track geometry, integration and power control on the charging performance. Accordingly, this paper proposes a design scheme for EV roadway powering systems, by synthetically analyzing the characteristics of dynamic charging. Based on the conducted analyzing results and proposed design scheme, it can offer a roadway powering system for EVs with salient advantages of the position-tolerant charging, constant energization, flexible power control, and cost saving.

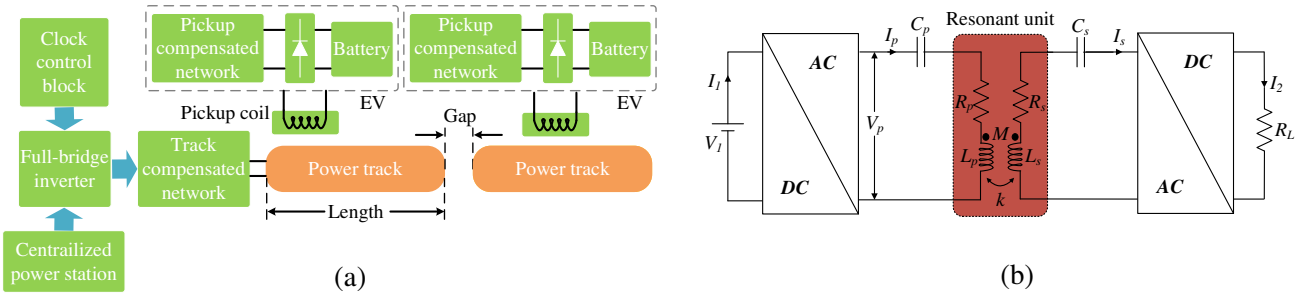


**Figure 1.** (a) Basic block diagram; (b) Equivalent circuit model.

## 2. ANALYSIS

The roadway powering system can constantly energize moving EVs, where the energy is cordlessly transmitted via the electromagnetic field induced by powering coils buried beneath the ground. Undoubtedly, the dynamic charging mechanism can significantly reduce the dependence on the battery for EVs, thus effectively increasing the driving range and saving the energy consumption as well as the cost. Technically, as shown in Fig. 1(a), the roadway powering system consists of three main units, the power supply to offer the AC power with the desired frequency, the compensation network to adjust the reactive power, and the track to induce the electromagnetic field. In the second unit, the pickup coil is also essential to be mounted inside EVs to collect the energy. Then, by adopting power electronic converters, the energy is further regulated to charge the battery or directly energize the electric motor.

In order to illustrate the working principle, Fig. 1(b) shows a single-phase circuit diagram for EV roadway powering systems. The primary current $I_p$ can be obtained as:

$$I_p = \frac{V_p}{Z_Q} \tag{1}$$

where $V_p$ is the primary voltage. Additionally, denote $Z_Q$ as the total impedance of the system, which can be calculated as:

$$Z_Q = \left[R_p + j\left(\omega L_p - \frac{1}{\omega C_p}\right)\right] + \frac{\omega^2 M^2}{R_s + R_L + j\left(\omega L_s - \frac{1}{\omega C_s}\right)} \tag{2}$$

Then, $\omega$ is the operating angular frequency, $R_L$ the equivalent resistance of the load, and $M$ the mutual inductance between the track and pickup coil as given by [16]:

$$M = k\sqrt{L_p L_s} \tag{3}$$

where $k$ is the coupling coefficient. In addition, $R_p$ and $R_s$ are the resistances of the track and pickup coil, respectively. $L_p$ and $L_s$ are the inductances of the track and pickup coil, respectively. $C_p$ and $C_s$ are the compensated capacitances of the primary and secondary units, respectively.

In the secondary unit, the current $I_s$ can also be calculated as [16]:

$$I_s = \frac{j\omega M \cdot I_p}{Z_s} \tag{4}$$

$Z_s$ is the impedance of the secondary pickup coil, which can be obtained as [16]:

$$Z_s = R_s + R_L + j\left(\omega L_s - \frac{1}{\omega C_s}\right) \tag{5}$$

Accordingly, the efficiency can be obtained as [3]:

$$\eta = \frac{\lambda}{\left(1 + \sqrt{1+\lambda}\right)^2} \tag{6}$$

where $\lambda$ is an intermediate variable as given by:

$$\lambda = k^2 Q_{p\_coil} Q_{s\_coil} \tag{7}$$

Denote the qualify factors of the primary and secondary coils as $Q_{p\_coil}$ and $Q_{s\_coil}$, which can be calculated as:

$$Q_{p\_coil} = \frac{\omega L_p}{R_p} \tag{8}$$

$$Q_{s\_coil} = \frac{\omega L_s}{R_s} \tag{9}$$

Consequently, it is shown that the transmission efficiency is significantly affected by the single track geometry, such as length, width and turns. Specifically, the track geometry determines the self-inductance, such as $L_p$ and $L_s$. Then, the quality factor, including $Q_{p\_coil}$ and $Q_{s\_coil}$, can be varied due to the variation of the self-inductance as expressed in Eqs. (8) and (9). According to Eq. (6), the transmission efficiency can be obtained by adjusting the parameters of the power track. In addition, the gap between adjacent tracks significantly affects the corresponding energy density. Besides, the power control is another major concern for the design of EV dynamic charging systems. Although the energy control can be effectively enriched by increasing power electronic converters, the negative effects are inevitably raised in terms of the increased switching loss, power density and installation cost. Thus, the design needs a reasonable tradeoff by systematically considering various performance indexes.

## 3. DESIGN

In this paper, a design scheme is proposed and implemented for the dynamic wireless charging system of roadway-powered electric vehicles, which focuses on track design to improve the transmission efficiency, integration to enhance the dynamic charging stability, and power control to enrich the energy management flexibility.

### 3.1. Track Design

As an energizing unit of roadway powering systems, the geometry of the track directly affects the wireless charging performances, especially for the power and efficiency. Then, the first design criterion is to offer enough power for the load, which can be mathematically expressed as:

$$P_s \geq P_L \tag{10}$$

where $P_L$ is the desired power. Additionally, $P_s$ is the pickup power which is given by [17]:

$$P_s = \omega I_p^2 \frac{M^2}{L_s} Q_s \tag{11}$$

Denote $Q_s$ is the qualify factor of the secondary circuit which can be obtained as:

$$Q_s = \frac{\omega L_s}{R_s + R_L} \tag{12}$$

By substituting Eqs. (3) and (12) into Eq. (11), the pickup power can be expressed as:

$$P_s = \omega^2 I_p^2 \frac{k^2 L_p L_s}{R_s + R_L} \tag{13}$$

On the other hand, it is known that $L_p$ is supposed to be proportional to the square of the number of turns $N$. According to Eq. (13), $P_s$ is proportional to $L_p$ so as to $N^2$. Then, the key is to find the minimum turns by increasing the number of turns until Equation (10) is satisfied.

As the most salient difference from the static wireless charging system, the EV dynamic charging has to take into account the impact of moving vehicles on the charging performance. It means that the designed roadway-powering system needs to continuously energize the vehicle for each predefined time slot ($\Delta T$). Accordingly, the minimum distance for continuous charging can be calculated as:

$$d_{\min} = V \Delta T \tag{14}$$

Denote the average velocity of EVs as $V$, which can be calculated based on the traffic flow. Then, the corresponding total cable length can be given by:

$$l_{cable} = 2N\left(\frac{d_{\min}}{n} + w_{track}\right) \cdot n = 2N d_{\min} + 2N \cdot n \cdot w_{track} \tag{15}$$

where $n$ is the number of tracks mounted in the minimum charging length. It is shown that the minimum $l_{cable}$ can be achieved by choosing $n = 1$, which means that the design can effectively reduce the installation cost, especially for copper materials. Thus, $l_{track}$ can be determined according to $d_{\min}$.

Accordingly, it means that the proposed design criteria can determine the minimum $l_{track}$ and $N$, so as to continuously feed the desired energy for EVs in each predefined time slot. Meanwhile, the internal resistance of the power track can be minimized, thus effectively reducing the power loss while providing the desired power for EVs.

### 3.2. Integration

In order to increase the dynamic charging stability, the uniform distribution of the induced electromagnetic field is required to realize the constant wireless charging for roadway-powered EVs. However, due to the inevitable interaction between adjacent tracks, the relative displacement significantly affects the charging performance, especially around the jointing area of power tracks. As we know, the induced magnetic field intensity is determined by the excitation current, namely in the direction proportional to $I_p$, the magnetic flux density $B$ can be expressed as:

$$B = h(I_p) \tag{16}$$

In order to assess the distribution of induced electromagnetic field, accordingly, this paper defines the magnetic distribution variance $D_{magnet}$, which is given by:

$$D_{magnet} = \sqrt{\frac{\left[h\left(I_{p1}\right) - B_{avg}\right]^2 + \cdots + \left[h\left(I_{pK}\right) - B_{avg}\right]^2}{K}} \tag{17}$$

where $h(I_{p1}) \ldots h(I_{pK})$ are the magnetic field intensity; $K$ is the number of sample points; $B_{avg}$ is the average magnetic flux density. Then, the roadway powering system needs to possess low variance $D_{magnet}$ indicating the even distribution of the induced electromagnetic field. Thus, the gap $d_{gap}$ can be determined based on the proposed definition of the distribution variance for the induced magnetic field.

### 3.3. Power Control

Apart from the track design and integration, the power control is also a major concern for enhancing the charging performance for roadway-powering systems. Ideally, each power track should be individually controlled by a single power converter, whereas it not only deteriorates the implement ability and the maintainability, but also increases the switching loss and construction cost. On the contrary, if all tracks are controlled by using only one power converter, the DC-link current will be inevitably increased and the control flexibility energy management deteriorated. Thus, this paper proposes a sectional power control scheme for roadway powering systems, where the tracks are grouped in a parallel connection. The number of tracks in a single group can be determined based on the system requirement and traffic flow. The corresponding scheme is elaborately discussed as below.

Technically, the rated current of the DC-link $I_{rated}$ is determined by the adopted power wire. Denote the average charging current for a single EV as $I_{avg}$. Due to the parallel connection adopted for grouping tracks, the allowed maximum number of vehicles in a single group can be expressed as:

$$n_{vehicle} = \frac{I_{rated}}{I_{avg}} \tag{18}$$

For moving vehicles, the actual occupied space of a single EV is determined by the vehicle length and safety distance. The average vehicle velocity $V$ can be calculated based on the traffic flow. Besides, the human average response time $T_{response}$ can be statistically estimated as 0.6 s [18]. Then, the safety distance $d_{safety}$ can be obtained as:

$$d_{safety} = VT_{response} \tag{19}$$

In such ways, the equivalent length $d_{vehicle}$ of a single moving EV can be obtained as:

$$d_{vehicle} = d_{safety} + l_{vehicle} \tag{20}$$

where $l_{vehicle}$ is the vehicle length. Thus, the section length $l_{section}$ is given by:

$$l_{\mathrm{sec}\,tion} = d_{vehicle} n_{vehicle} \tag{21}$$

Thus, the number of tracks in a single section $n_{section}$ can be obtained by:

$$n_{\mathrm{sec}\,tion} = floor\left(\frac{l_{\mathrm{sec}\,tion}}{l_{track} + d_{gap}}\right) \tag{22}$$

where $floor(\cdot)$ is the rounding function.

## 4. VERIFICATION

In this paper, the feasibility of the proposed design of dynamic wireless charging systems is verified for roadway-powered EVs by carrying out the JMAG-based electromagnetic field analysis as well as the MATLAB-based circuit simulation. In addition, the experimental prototype is also set up to further demonstrate the proposed design scheme. Corresponding key parameters are listed in Table 1.

### 4.1. Simulation Results

According to the EV dynamic wireless charging system, the exemplified setup mainly consists of power track, pickup coil, compensation network, and power electronic converters. Based on the proposed analysis and design procedure, the parameters of the exemplified roadway powering system can be obtained. Fig. 2(a) depicts the dimensions of power tracks, where the windings are distributed unevenly with the number of turns of 5, 4, 3, 2, respectively. The adopted unevenly-distributed winding scheme can induce a smooth magnetic field so as to ensure the continuous charging for EVs. By adopting the proposed design scheme, as shown in Fig. 2(b), the length, width and gap of power tracks are chosen as 14 m, 3.5 m and 0.9 m, respectively. In addition, the total length of the exemplified roadway powering system is 45 m. Besides, the verification adopts operating frequency of 20 kHz. The corresponding compensated capacitances of the power track and pickup coil are chosen as $6.75\times10^{-7}$ F and $267\times10^{-7}$ F, respectively.

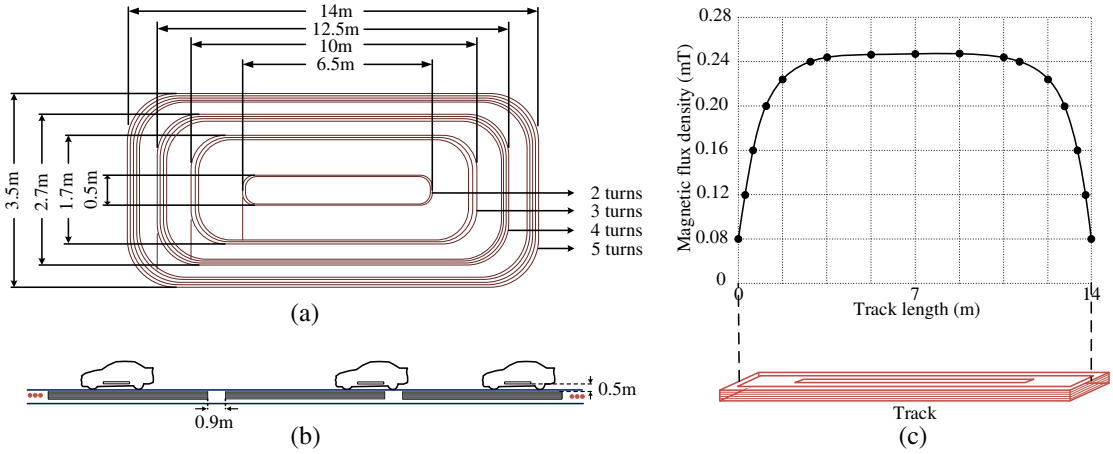


**Figure 2.** (a) Geometry of exemplified roadway powering system; (b) Gaps of exemplified roadway powering system; (c) Simulated magnetic flux density.

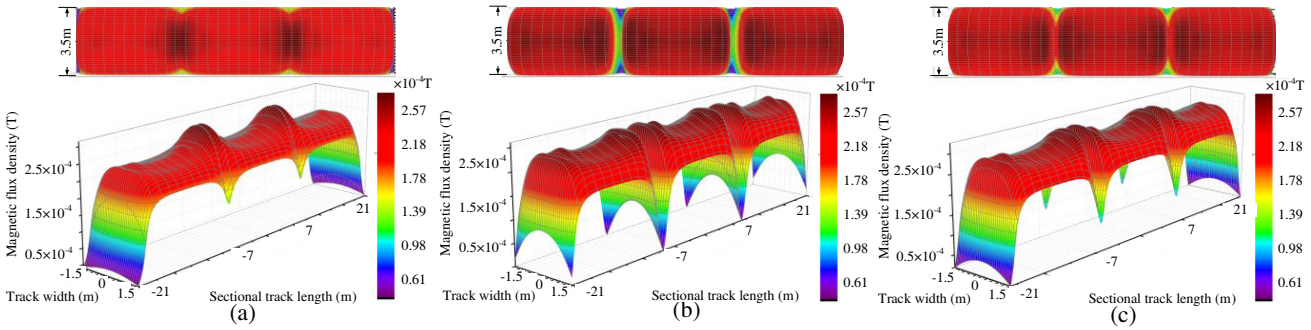


**Figure 3.** Comparative analysis of electromagnetic field distribution: (a) 0.5 m; (b) 1.3 m; (c) 0.9 m.

Figure 2(c) shows the simulated results of the electromagnetic field above a single power track with the distance of 0.5 m, which equals the power transmission distance in the verification. The magnetic flux density can reach around 0.24 mT. Besides, the corresponding charging voltage can successfully achieve EV's rated power, which is capable of energizing the EVs in the actual verification. Thus, it is shown that the proposed design scheme can effectively induce the electromagnetic field with a desired strength to offer enough power for involved moving EVs as well as an even distribution for the constant energization.

By adopting three different gap values, comparative analysis is carried out to verify the effectiveness of the proposed design criteria for the gap between adjacent power tracks. Fig. 3(a) shows that a small gap (0.5 m) produces a over-concentrated distribution around the jointing area of adjacent power tracks. It strengthens the mutual effect due to the increased coupling coefficient, thus inevitably increasing the power loss. It also results in additional construction cost due to increased power tracks. Fig. 3(b) shows that a large gap (1.3 m) significantly deteriorates the electromagnetic field distribution, even resulting in energy vacuum in specific areas. According to the proposed design scheme, the gap is chosen as 0.9 m. Fig. 3(c) shows that the electromagnetic field is distributed smoothly and uniformly over the jointing area of adjacent powering tracks, which means that the moving EV can be constantly energized everywhere on the road. Fig. 4 shows the corresponding simulated magnetic flux density along the road central line, where the small gap produces the peak around 0.28 mT, and the large gap makes the magnetic flux density dramatically dropped to below 0.12 mT over the jointing area. Thus, it further illustrates the salient advantages of the proposed design criteria. Besides, the corresponding magnetic distribution variance is also calculated as shown in Fig. 5(a), which equals 0.0000207 (0.5 m), 0.0000299 (1.3 m), and 0.0000191 (0.9 m). Obviously, the adopted gap possesses the lowest variance value, which

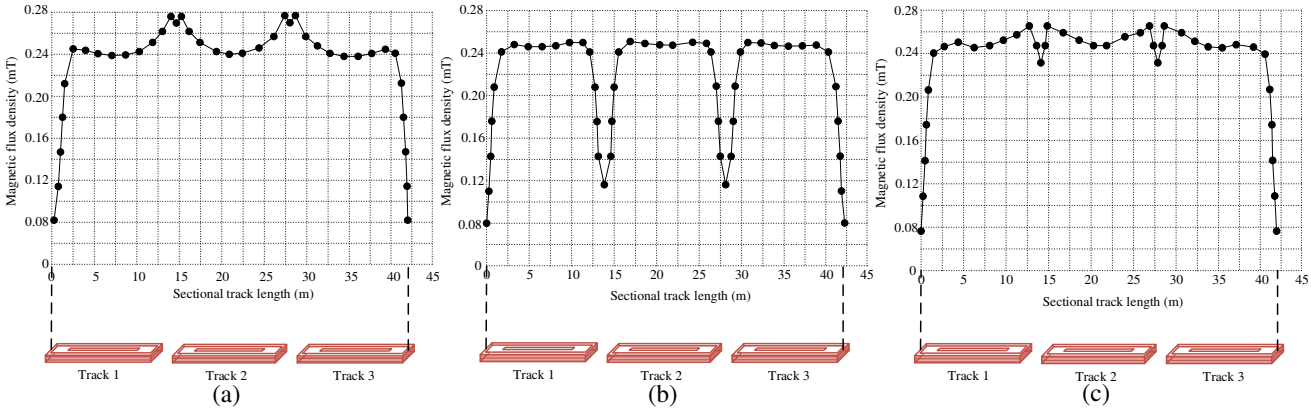


**Figure 4.** Simulated magnetic flux density: (a) 0.5 m; (b) 1.3 m; (c) 0.9 m.

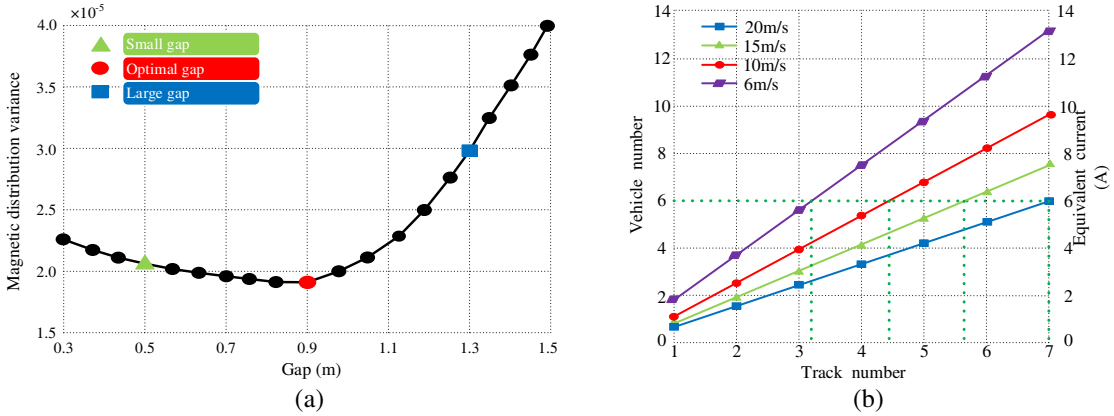


**Figure 5.** (a) Magnetic distribution variance versus displacement; (b) Design criteria for proposed power section.

also illustrates that the proposed design scheme can successfully offer the desired evenly-distributed electromagnetic field.

According to Eq. (22), the number of tracks can be selected as depicted in Fig. 5(b), where the relationship between the traffic flow and section length is plotted by selecting various velocities, such as 6 m/s, 10 m/s, 15 m/s, and 20 m/s in the exemplification. Assume that the charging current is 1 A with respect to a single vehicle and that the maximum DC-link current is 6 A in the adopted computational simulation. Then, the maximum vehicle can be calculated based on Eq. (18), namely $n_{vehicle}$, equals 6 as indicated by the green dotted line. As a result, the maximum number of power tracks can be determined based on the traffic flow for a single section. For example, the maximum number of tracks should be 4, 5, 6, and 7 with respect to the average velocity of as 6 m/s, 10 m/s, 15 m/s, and 20 m/s.

### 4.2. Experimental Results

To experimentally demonstrate the proposed design scheme for EV dynamic charging systems, the conducted scale-down experimental prototype is set up as shown in Fig. 6(a). The corresponding key parameters are listed in Table 1. Bulbs are used to replace EVs, and brightness level represents the amount of received energies. The power source is provided by a DC power supply. DSP controller is used, and the transient currents are sensed by Honeywell sensors (LA25-NP). All measured waveforms are fed into a light oscilloscope.

Figure 6(b) shows the distribution of the induced voltage on the horizontal plane above the power track with a height of 0.2 m, namely the pickup-located plane, which is obtained by measuring the

**Table 1.** Parameters of three coils.

| Item | Inductance (mH) | Resistance (Ω) | Length (m) | Width (m) | Q | k |
|---|---|---|---|---|---|---|
| Power track 1 | 0.09752 | 0.2114 | 0.65 | 0.20 | 57.94 | 0.10 |
| Power track 2 | 0.09811 | 0.2196 | 0.65 | 0.20 | 56.11 | 0.009 |
| Power track 3 | 0.09698 | 0.2061 | 0.65 | 0.20 | 59.10 | 0.011 |

voltage of pickup coils. It illustrates that the voltage can be evenly distributed over the whole power track with the value around 13 V. In addition, compared with the right bulb in Fig. 6(a), the minimum number of track turns can effectively offer enough energy for the middle bulb with the specific power supply. Thus, it experimentally verifies the effectiveness of the proposed track design scheme. Fig. 7 shows the measured voltage waveforms of power track and pickup coil. Fig. 8 shows the measured voltage waveforms of Honeywell sensor which can indicate current value indirectly. Fig. 8(b) shows the waveform with exemplified bulb located in the jointing area between adjacent power tracks. It does not appear much different from that in Fig. 8(a). Accordingly, it illustrates that the proposed integration scheme can successfully reduce the drop of the magnetic flux density caused by the counteraction between power tracks.

Thus, the experimental results agree well with the theoretical analysis and simulation results. It is verified that the proposed design scheme can effectively offer the desired power for bulbs as well as involved moving EVs, successfully ensure the control flexibility for the energy management, and significantly reduce the power loss as well as the construction cost.

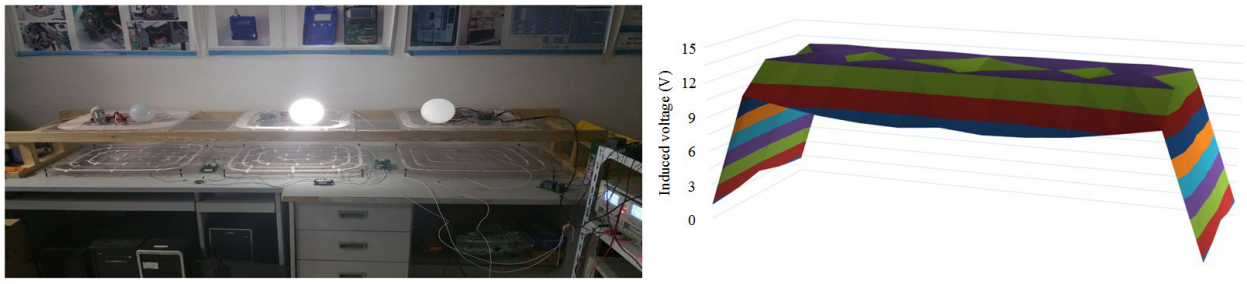


(a) (b)

**Figure 6.** (a) Experimental prototype; (b) Measured electromagnetic field induced by proposed track.

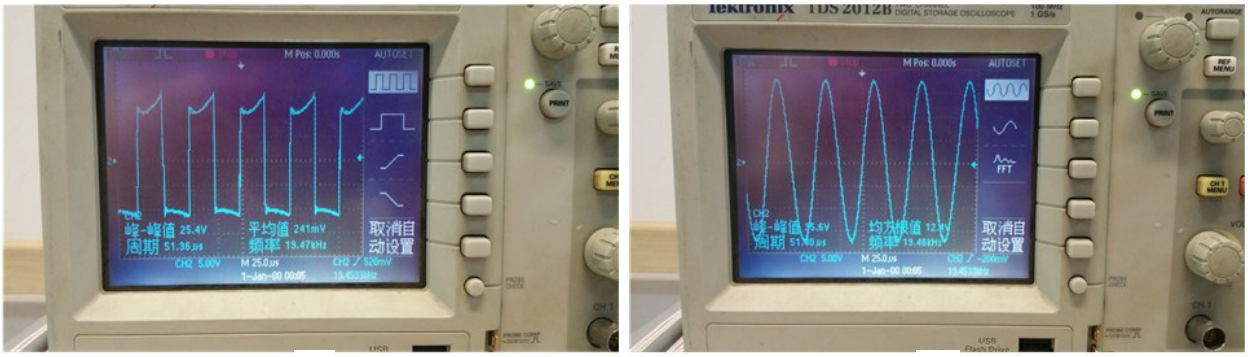

(a) (b)

**Figure 7.** Measured voltage waveforms: (a) power track ($X$: 25 µs/div, $Y$: 5 V/div); (b) pickup coil ($X$: 25 µs/div, $Y$: 5 V/div).


(a) (b)

**Figure 8.** Measured voltage waveforms of Honeywell sensor: (a) right above the power track ($X$: 25 µs/div, $Y$: 500 mV/div); (b) right above the gap ($X$: 25 µs/div, $Y$: 500 mV/div).

## 5. CONCLUSION

By synthetically analyzing the roadway powering system, this paper has revealed the key factors, such as the track geometry, interaction between adjacent tracks, and power electronic converter, which affects the dynamic charging performances for EVs. Then, the design scheme has been proposed from the perspective of the track design, integration and power control, respectively. Specifically, the length and number of turns can be designed based on the power supply and demand as well as the loss. Then, the gap between adjacent power tracks can be determined by minimizing the proposed magnetic distribution variance. In addition, the sectional control has been proposed to enhance the control flexibility for the energy management, where the number of tracks can be calculated based on the maximum DC-link current and traffic flow. Both the simulated and experimental results have validated that the proposed design scheme can effectively offer the desired power, enhance the control flexibility, and reduce the power loss as well as the construction cost for EV dynamic charging systems.

## ACKNOWLEDGMENT

This work was supported by the National Natural Science Foundation of China (Grant No. 51607120) and the Natural Science Foundation of Tianjin, China (Grant No. 16JCQNJC01500).

## REFERENCES

1. Chau, K. T., *Electric Vehicle Machines and Drives — Design, Analysis and Application*, Wiley-IEEE Press, 2015.
2. Covic G. A. and J. T. Boys, "Inductive power transfer," *Proc. IEEE*, Vol. 101, 1276–1289, 2013.
3. Guo, Y., L. Wang, and C. Liao, "Systematic analysis of conducted electromagnetic interferences for the electric drive system in electric vehicles," *Progress In Electromagnetics Research*, Vol. 134, 359–378, 2013.
4. Poon, A. S. Y., "A general solution to wireless power transfer between two circular loop," *Progress In Electromagnetics Research*, Vol. 148, 171–182, 2014
5. Robichaud, A., M. Boudreault, and D. Deslandes, "Theoretical analysis of resonant wireless power transmission links composed of electrically small loops," *Progress In Electromagnetics Research*, Vol. 143, 485–501, 2013
6. Wang, C. S., O. H. Stielau, and G. A. Covic, "Design consideration for a contactless electric vehicle battery charger," *IEEE Trans. Ind. Electron.*, Vol. 52, 1308–1313, 2005.
7. Budhia, M., J. T. Boys, G. A. Covic, and C. Y. Huang, "Development of a single-sided flux magnetic coupler for electric vehicle IPT charging systems," *IEEE Trans. Ind. Electron.*, Vol. 60, 2013.

8. Deng, J. J., F. Lu, S. Q. Li, T. D. Nguyen, and C. Mi, "Development of a high efficiency primary side controlled 7 kW wireless power charger," *Proceedings of IEEE International Electric Vehicle Conference*, Vol. 16, 2014.
9. Hasanzadeh, S., S. V. Zadeh, and A. H. Isfahani, "Optimization of a contactless power transfer system for electric vehicles," *IEEE Trans. Veh. Technol.*, Vol. 61, 3566–3573, 2012.
10. Choi, S., J. Huh, W. Y. Lee, S. W. Lee, and C. T. Rim, "New cross-segmented power supply rails for roadway-powered electric vehicles," *IEEE Trans. Power Electron.*, Vol. 28, 5832–5841, 2013.
11. Choi, S. Y., S. Y. Jeong, E. S. Lee, B. W. Gu, S. W. Lee, and C. T. Rim, "Generalized models on self-decoupled dual pick-up coils for large lateral tolerance," *IEEE Trans. Power Electron.*, Vol. 30, 6434–6445, 2015.
12. Ibrahim, M., L. Pichon, L. Bernard, A. Razek, J. Houivet, and O. Cayol, "Advanced modeling of a 2-kW series–series resonating inductive charger for real electric vehicle," *IEEE Trans. Veh. Technol.*, Vol. 64, 421–430, 2015.
13. Albesa, J. and M. Gasulla, "Occupancy and belt detection in removable vehicle seats via inductive power transmission," *IEEE Trans. Veh. Technol.*, Vol. 64, 3392–3401, 2015.
14. Jeong, S., Y. J. Jang, and D. Kum, "Economic analysis of the dynamic charging electric vehicle," *IEEE Trans. Power Electron.*, Vol. 30, 6368–6377, 2015.
15. Shun, J., S. Shin, Y. Kim, S. Ahn, S. Lee, G. Jung, S. J. Jeon, and D. H. Cho, "Design and implementation of shaped magnetic-resonance-based wireless power transfer system for roadway-powered moving electric vehicles," *IEEE Trans. Ind. Electron.*, Vol. 61, 1179–1192, 2013.
16. Mutashar, S., M. A. Hannan, S. A. Samad, and A. Hussain, "Analysis and optimization of spiral circular inductive coupling link for bio-implanted applications on air and within human tissue," *Sensors*, Vol. 14, No. 7, 11522–11541, 2014.
17. Covic, G. A. and J. T. Boys, "Morden trends in inductive power transfer for transportation applications," *IEEE Trans. Emerging Sel. Topics Power Electron*, Vol. 1, 2841, 2013.
18. Green, M., "How long does it take to stop? Methodological analysis of driver perception-brake times," *Transportation Human Factors*, Vol. 2, 195–216, 2000.